

Table 1. Summary of hypotheses, corresponding specific predictions, and results.

Hypotheses & Specific Predictions	Prediction supported?				Results
	recent non-drought conditions	tree-ring drought records			
		Resistance (Rt)	Recovery (Rc)	Resilience (Rs)	
Tree size and microenvironment					
<i>Across the forest vertical profile, taller trees are exposed to higher evaporative demand.</i>					
Taller trees experience higher wind speeds during the peak growing season months.	yes				Fig. 2
Taller trees experience lower humidity during the peak growing season months.	yes				Fig. 2
Taller trees experience higher air temperatures during the peak growing season months.	no				Fig. 2
Taller trees have more sun-exposed crowns.	yes				Fig. 2
<i>At least within the forest setting, taller trees are less drought tolerant.</i>					
Drought tolerance decreases with height (H).		yes	yes	yes	Fig. 4; Tables S8-S11
<i>Small trees (lower root volume) in drier microhabitats have lower drought tolerance.</i>					
There is a negative interactive effect between H and topographic wetness index.		(no)	(yes)	(yes)	Tables S8-S11
Species traits					
<i>Species' traits—particularly leaf drought tolerance traits—predict drought tolerance.</i>					
Wood density correlates (positively or negatively) to drought tolerance.		-	-	-	Tables S4-S7
Leaf mass per area correlates positively to drought tolerance.		-	-	-	Tables S4-S7
Ring-porous species have higher drought tolerance than diffuse- or semi-ring- porous.		-	no	-	Tables S4-S7
Percent loss leaf area upon desiccation correlates negatively with drought tolerance.		yes	(yes)	(yes)	Fig. 4; Tables S8-S11
Water potential at turgor loss correlates negatively with drought tolerance.		(yes)	(yes)	(yes)	Fig. 4; Tables S8-S11

Parentheses indicate that the prediction was supported by at least one but not all of the top models (Table S8). Dash symbols indicate that the response was not significant (Table S4), or not represented in any of the top models (Table S8).

Table 2. Overview of analyzed species, listed in order of their relative contributions to woody stem productivity ($ANPP_{stem}$) in the plot, along with numbers and sizes sampled, and species traits. Variable abbreviations are as in Table 3. DBH measurements are from the most recent ForestGEO census in 2018 (live trees) or tree mortality censuses in 2016 and 2017 (trees cored dead).

species	% $ANPP_{stem}$	n trees*	contemporary DBH (cm)		species traits (mean +/- se)				
			mean	range	WD ($g\ cm^{-3}$)	LMA ($g\ cm^{-2}$)	xylem porosity	π_{tlp} (Mpa)	PLA_{dry} (%)
Liriodendron tulipifera (LITU)	47.1	98	36.9	10 - 100.4	0.4 ± 0.03	46.9 ± 12.4	diffuse	-1.92 ± 0.17	19.6 ± 2.06
Quercus alba (QUAL)	10.7	61	47.2	11.4 - 79.1	0.61 ± 0.02	75.8 ± 11.1	ring	-2.58 ± 0.08	8.52 ± 0.37
Quercus rubra (QURU)	10.1	69	54.9	11.1 - 148	0.62 ± 0.02	71.1 ± 6.70	ring	-2.64 ± 0.28	11.0 ± 0.84
Quercus velutina (QUVE)	7.8	77	54.1	16.0 - 114.2	0.65 ± 0.04	48.7 ± 3.30	ring	-2.39 ± 0.15	13.42 ± 0.84
Quercus montana (QUPR)	4.8	59	42.3	10.5 - 87.2	0.61 ± 0.01	71.8 ± 40.2	ring	-2.36 ± 0.09	11.75 ± 1.37
Fraxinus americana (FRAM)	3.8	62	35.4	6.4 - 94.7	0.56 ± 0.01	43.3 ± 4.78	ring	-2.1 ± 0.36	13.06 ± 1.06
Carya glabra (CAGL)	3.7	31	31.4	9.8 - 98.5	0.62 ± 0.04	42.8 ± 0.94	ring	-2.13 ± 0.50	21.09 ± 5.48
Juglans nigra (JUNI)	2.1	31	48.1	24.2 - 87	1.09 ± 0.09	72.1 ± 7.10	semi-ring [†]	-2.76 ± 0.21	24.64 ± 8.72
Carya cordiformis (CACO)	2.0	13	27.2	10.7 - 61.5	0.83 ± 0.10	45.9 ± 15.6	ring	-2.13 ± 0.45	17.22 ± 2.25
Carya tomentosa (CATO)	2.0	13	21.0	12.1 - 32.2	0.83	45.4	ring	-2.2	16.56
Fagus grandifolia (FAGR)	1.5	80	23.5	11.2 - 107.2	0.62 ± 0.03	30.7 ± 4.94	diffuse	-2.57	9.45 ± 1.25
Carya ovalis (CAOVL)	1.1	23	35.3	14.9 - 66.0	0.96 ± 0.33	47.6 ± 3.95	ring	-2.48 ± 0.04	14.8 ± 6.34

* Numbers cored live versus dead are given in Table S1 of Helcoski et al. (2019).

[†] Semi-ring porosity is intermediate between ring and diffuse. We group it with diffuse-porous species for more even division of species between categories.

Table 3. Summary of dependent and independent variables in our statistical models of drought tolerance, along with units, definitions, and sample sizes.

variable	symbol	units	description	category	n_{Rt}^*	n_{Rc}	n_{Rs}
Dependent variables							
drought resistance	Rt	-	ratio of growth during drought year to mean growth of the 5 years prior.	-	1623	-	-
	Rt_{ARIMA}	-	ratio of growth during drought year to growth predicted by ARIMA model.	-	1654	-	-
drought recovery	Rc	-	ratio of mean growth for 5 years after drought to growth during year.	-	-	1557	-
drought resilience	Rs	-	ratio of mean growth for 5 years after drought to mean growth for 5 years before drought.	-	-	-	1570
Independent variables							
drought year	Y	-	year of drought	1966	513	491	495
				1977	543	524	523
				1999	567	542	552
height	H	m	estimated H in drought year	-	-	-	-
topographic wetness index	TWI	-	steady-state wetness index based on slope and upstream contributing area	-	-	-	-
<i>species' traits</i>							
wood density	WD	g cm^{-3}	dry mass of a unit volume of fresh wood	-	-	-	-
leaf mass per area	LMA	kg m^{-2}	ratio of leaf dry mass to fresh leaf area	-	-	-	-
xylem porosity		-	vessel arrangement in xylem	ring (R)	1106	1079	1088
				semi-ring (SR)	81	73	78
				diffuse (D)	436	405	404
turgor loss point	π_{tlp}	MPa	water potential at which leaves wilt	-	-	-	-
percent loss area	PLA_{dry}	%	percent loss of leaf area upon dessication	-	-	-	-

Sample sizes are after removal of outliers. Dashes for sample sizes of independent variables indicate that the variable was available for all records. Xylem porosity sample sizes are sums across all drought years.

*Sample sizes of independent variables refer to the Rt model.

Figure Legends

Figure 1. Climate and species-level growth responses over our study period, highlighting the three focal droughts (a) and community-wide growth resistance, R_t (b), and resilience, R_s (c). Time series plot (a) shows peak growing season (May-August) climate conditions and residual chronologies for each species (see Table 3 for codes). PET and PRE data were obtained from the Climatic Research Unit high-resolution gridded dataset (CRU TS v.4.01; Harris et al. 2014). Focal droughts are indicated by dashed lines, and shading indicates the pre- and post- drought periods used in calculations of the resistance metric. Figure modified from Helcoski *et al.* (2019). Density plots (b-c) show the distribution of R_t and R_s values for each drought. See Fig. S6 for parallel plot for recovery (R_c).

Figure 2. Contemporary height profiles in sun exposure and growing season microclimate under non-drought conditions. Shown are average (\pm SD) of daily maxima and minima of (a) wind speed, (b) relative humidity (RH), and (c) air temperature (T_{air}) averaged over each month of the peak growing season (May-August) from 2016-2018. In these plots, heights are slightly offset for visualization purposes. Asterisks indicate significant differences between the top and bottom of the height profile. Also shown is (d) tree heights by 2018 crown position, with letters indicating significance groupings. In all plots, the dashed horizontal line indicates the 95th percentile of tree heights in the ForestGEO plot.

Figure 3. Drought resistance, R_t (a), and resilience, R_s (b), across species for the three focal droughts. Species codes are given in Table 2. See Fig. S7 for parallel plot for recovery (R_c).

Figure 4. Visualization of best statistical models for drought resistance (R_t), recovery (R_c), and resilience (R_s) for all droughts combined and for each individual drought year. Confidence intervals were defined via bootstrapping in the bootpredictlme4 package. Model coefficients are given in Tables S8 and S10-11.

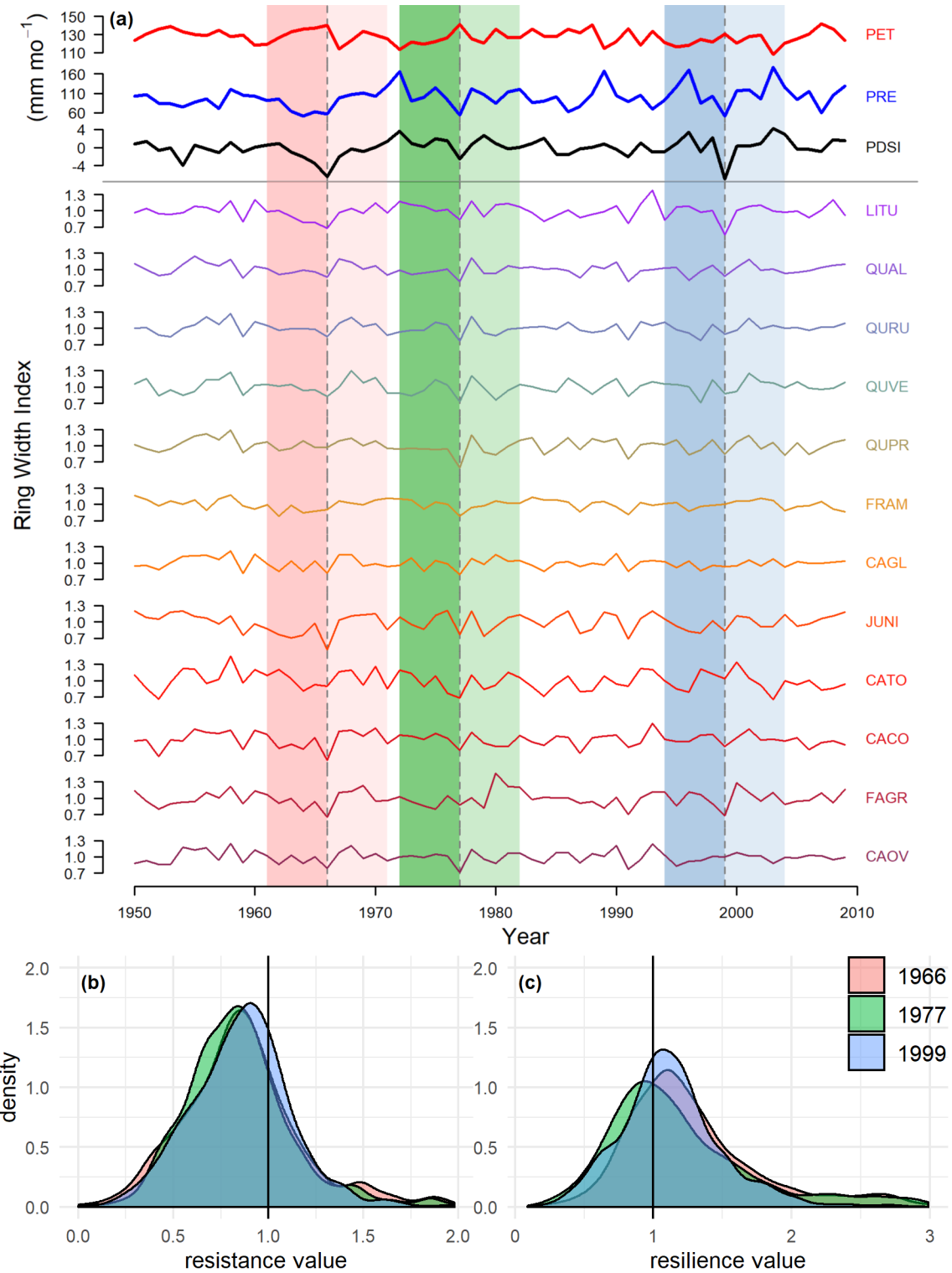


Figure 1. Climate and species-level growth responses over our study period, highlighting the three focal droughts (a) and community-wide growth resistance, R_t (b), and resilience, R_s (c). Time series plot (a) shows peak growing season (May–August) climate conditions and residual chronologies for each species (see Table 3 for codes). PET and PRE data were obtained from the Climatic Research Unit high-resolution gridded dataset (CRU TS v.4.01; Harris *et al.* 2014). Focal droughts are indicated by dashed lines, and shading indicates the pre- and post-drought periods used in calculations of the resistance metric. Figure modified from Helcoski *et al.* (2019). Density plots (b–c) show the distribution of R_t and R_s values for each drought. See Fig. S6 for parallel plot for recovery (R_c).



Figure 2. Contemporary height profiles in sun exposure and growing season microclimate under non-drought conditions. Shown are average (\pm SD) of daily maxima and minima of (a) wind speed, (b) relative humidity (RH), and (c) air temperature (T_{air}) averaged over each month of the peak growing season (May-August) from 2016-2018. In these plots, heights are slightly offset for visualization purposes. Asterisks indicate significant differences between the top and bottom of the height profile. Also shown is (d) tree heights by 2018 crown position, with letters indicating significance groupings. In all plots, the dashed horizontal line indicates the 95th percentile of tree heights in the ForestGEO plot.

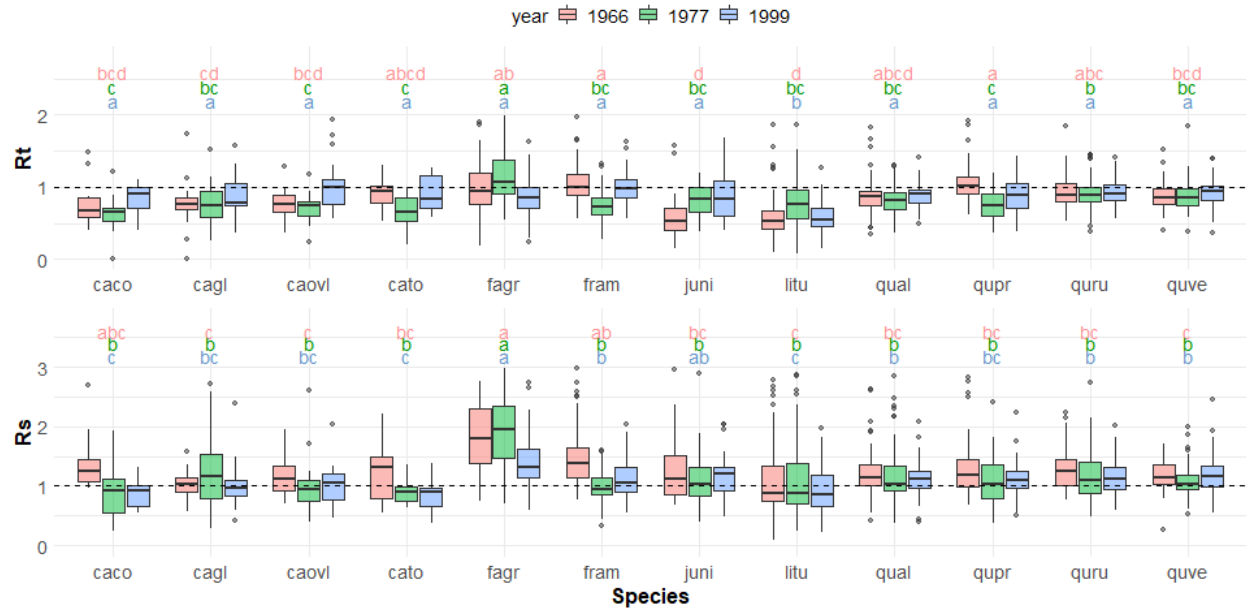


Figure 3. Drought resistance, R_t (a), and resilience, R_s (b), across species for the three focal droughts. Species codes are given in Table 2. See Fig. S7 for parallel plot for recovery (R_c).

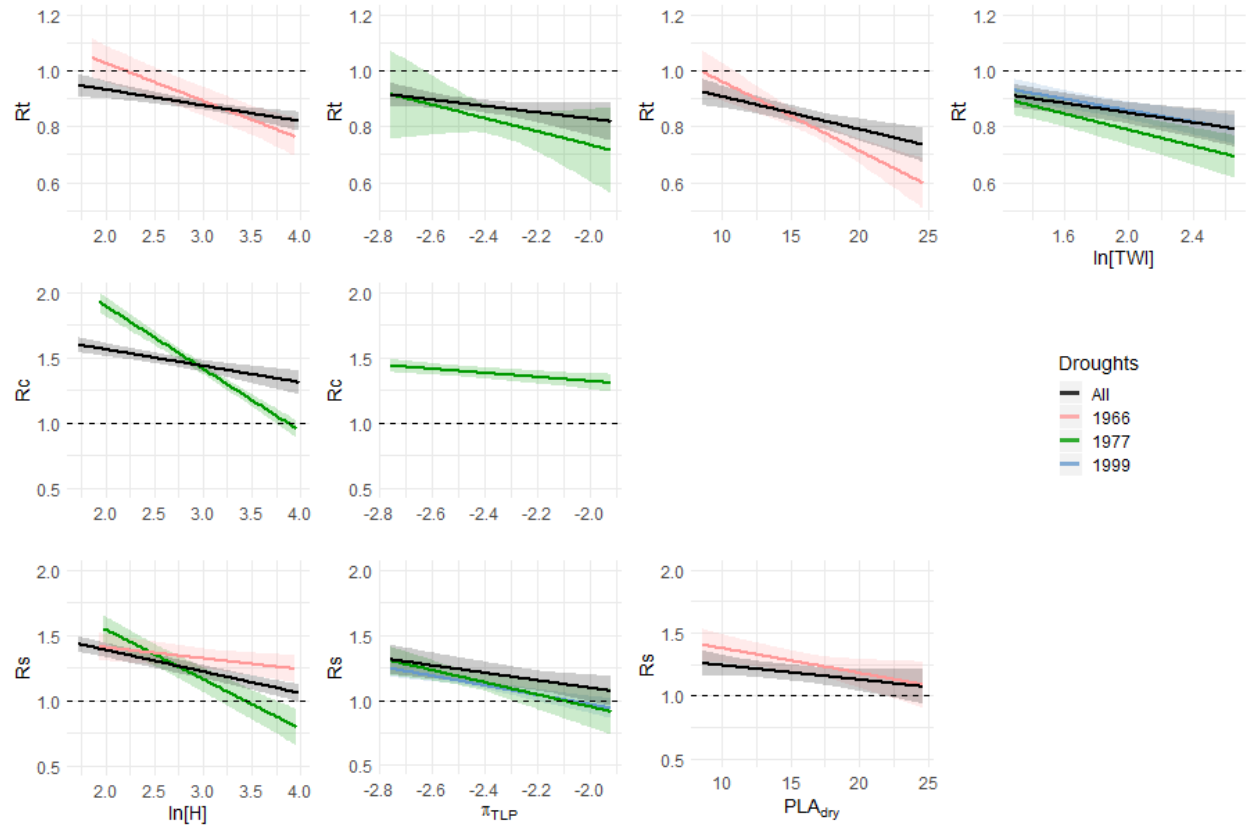


Figure 4. Visualization of best statistical models for drought resistance (R_t), recovery (R_c), and resilience (R_s) for all droughts combined and for each individual drought year. Confidence intervals were defined via bootstrapping in the bootpredictlme4 package. Model coefficients are given in Tables S8 and S10-11.